

COLOR IMAGE CLASSIFICATION SYSTEMS FOR POULTRY VISCERA INSPECTION

K. Chao, Y. R. Chen, H. Early, B. Park

ABSTRACT. A neuro-fuzzy based image classification system that utilizes color-imaging features of poultry viscera in the spectral and spatial domains was developed in this study. Color images of 320 livers and hearts from normal, airsacculitis, cadaver, and septicemia chickens were collected in the poultry process plant. These images in red, green, and blue (RGB) color space were segmented and statistical analysis was performed for feature selection. A neuro-fuzzy system utilizing hybrid paradigms of fuzzy inference system and neural networks was used to enhance the robustness of the classification processes. The accuracy for separation of normal from abnormal livers ranged 87.5 to 92.5%, when two classes of validation data were used. For classification of normal and abnormal chicken hearts, the accuracies were 92.5 to 97.5%. When neuro-fuzzy models were employed to separate chicken livers into normal, airsacculitis, and cadaver, the accuracy was 88.3% for the training data and 83.3% for the validation data. Combining features of chicken liver and heart, a generalized neuro-fuzzy model was designed to classify poultry viscera into four classes (normal, airsacculitis, cadaver, and septicemia). The classification accuracy was 86.3% for training and 82.5% for validation.

Keywords. Automation, Food safety, Fuzzy logic, Machine vision, Pattern recognition.

Poultry and poultry products have increased in popularity with U.S. consumers in recent years. With an increased demand for poultry products, food safety becomes an increasingly important issue. The practical application of food microbiology in poultry processing and marketing can be used to ensure clean, wholesome products from each carcass. However, under commercial production, processing, handling, and marketing conditions, it is not feasible to run microbiological counts (Mountney, 1987) to determine the presence or absence of pathogens on all birds handled. For this reason, current practice of poultry inspection in the processing plant is based on postmortem pathology correlation (e.g., observe signs of abnormalities or diseases from carcass exterior, body cavity, and viscera).

In modern poultry plants, USDA-certified inspectors perform the whole inspection process. Individual, high-speed visual inspection of birds (30 birds/min) is both labor intensive and prone to human error and variability. In the past five years, several studies have been reported on the developments of automated inspection systems for poultry carcass inspection (Chen and Massie, 1993; Chen et al.,

1996; Park and Chen, 1996). Two prototype systems using visible/near-infrared spectroscopy and multispectral imaging techniques are currently being developed at the Instrumentation and Sensing Laboratory, USDA, ARS, for on-line poultry carcass inspection.

Previous studies (Chen et al., 1998a; Park et al., 1998) have shown that the systems can separate normal poultry carcasses from abnormal carcasses. The system, however, may not be able to perfectly discriminate individual abnormal carcasses. In addition, procedures that only scan/image the carcass exteriors are insufficient to detect some condemned conditions such as airsacculitis and ascites. Thus, there is a need for acquiring additional feature information (using machine vision) from postmortem poultry at different positions (e.g., body cavity) and/or from different internal organs (e.g., liver and heart).

Feature identification and classification are two important tasks in machine vision applications. Color is an especially important attribute for food inspection (Daley et al., 1994; Tao et al., 1995). With the availability of improved hardware for acquiring color images and advances in soft computing (Jang 1993; Nauck and Kruse, 1995), capability now exists for development of color vision systems for poultry inspection. In this study the feasibility of a color imaging system to identify individual condemned conditions from poultry viscera inspection was investigated. Specifically, the objectives were to:

1. Determine features for discriminating condemned conditions of poultry viscera.
2. Develop the neuro-fuzzy models for identifying individual poultry viscera condemnations.

MATERIALS AND METHODS

SAMPLE PREPARATION

A total of 320 chicken livers and hearts (160 each) were collected from a poultry process plant in Pennsylvania in

Article was submitted for publication in October 1998; reviewed and approved for publication by the Information & Electrical Technologies Division of ASAE in May 1999.

Mention of company or trade names is for purpose of description only and does not imply endorsement by the U.S. Department of Agriculture.

The authors are **Kuanglin Chao, ASAE Member**, Research Scientist, **Yud-Ren Chen, ASAE Member Engineer**, Research Leader, Instrumentation and Sensing Laboratory, BARC, ARS, USDA, Beltsville, Md.; **Howard Early**, Veterinary Medical Officer, Technical Assessment Branch, FSIS, USDA, Washington, D.C.; and **Bosoon Park, ASAE Member Engineer**, Faculty Research Associate, Biological Resources Engineering Department, University of Maryland, College Park, Md. **Corresponding author:** Kuanglin Chao, USDA-ARS-ISL, Bldg. 303, BARC-East, 10300 Baltimore Avenue, Beltsville, MD 20705-2350; voice: (301) 504-8450; fax: 301-504-9466; e-mail: kchao@asrr.arsusda.gov.

April and August 1998. Samples of livers and hearts were inspected and collected by USDA Food Safety and Inspection Service veterinarians. These samples were separated into four-classes: airsacculitis, cadaver, normal, and septicemia based on the postmortem pathology findings from the veterinarians. Samples of the same class were placed in plastic bags and immediately moved to a nearby room for on-site color image measurement.

COLOR VISION SYSTEM

The color imaging system used in this study consisted of a 24-bit CCD color video camera (TMC-74, PULNiX America Inc., Sunnyvale, Calif.), a portable lighting chamber, and a frame-grabber board (IC-RGB, Imaging Technology Inc., Bedford, Mass.) installed in a 75 MHz Intel Pentium™ computer with 40 MB of memory running Microsoft Windows 95™. The portable lighting chamber was equipped with a Quartz Halogen lamp (EKE, 150W, 21V USHIO Inc., Tokyo, Japan) and a bundled fiber optic ring light (A3739P, Dolan-Jenner Industries, Inc., Lawrence, Mass.) to provide 360° diffuse illumination. An AC-regulated power supply unit (PL 800, Dolan-Jenner Industries, Inc., Lawrence, Mass.) equipped with solid state intensity control (0-100%) was used for stabilizing input line voltage. The camera was mounted perpendicular to the top plane of the illumination chamber. The AGC (Auto Gain Control) and AWB (Auto White Balance) of the color camera were turned off during image acquisition.

The vision sensor imaged a 17.4 cm × 13.9 cm field of view and, when calibrated, each pixel represented an area of 0.34 mm × 0.29 mm. The vision system was calibrated for spectral measurement before each imaging acquisition session. A color chart (ColorChecker, GretagMacbeth, New Windsor, N.Y.) was used as a standard reflectance reference for color calibration.

IMAGE PROCESSING

Individual poultry viscera (i.e., livers and hearts) were placed on a white Teflon sheet (25 × 25 × 0.3 cm) when images were taken. Image application software (Optimas 6.2, Optimas Corp., Bothell, Wash.) was used to process acquired images. The viscera images were processed for gray intensity measurements and morphological features. The threshold of a color image consists of a vector of high and low intensity ranges, one for each color space. Dynamic threshold values were derived interactively from intensity histograms of the images in each color space. The substantial reflectance difference between the samples (livers and hearts) and the white background allowed the simplification of the thresholding process. The average gray-level intensities of each liver in RGB color space were calculated with a user-defined script file. Two-stage segmentation was applied to process heart images. The heart image was first separated from the background by a simple threshold scheme. Once the heart image was segmented from the background, dynamic threshold values were applied to extract morphological features from the chicken heart.

FEATURE EXTRACTION

Color is an important feature for poultry viscera inspection. For example, cadaver and airsacculitis livers have distinguished color changes. The liver color from

cadaver carcasses is dark red because the carcasses were not properly bled out. A airsacculitis is commonly used to describe a respiratory syndrome in broiler chicken. The livers from airsacculitic carcasses have fibrinous coating firmly attached. Septicemia is a systemic disease caused by pathogenic microorganisms in the blood. Septicemia carcasses have various visible changes. The skin of septicemia carcasses is darkened red to bluish discoloration, while the internal organ, such as the heart, is dehydrated.

Two sets of features extracted from viscera images were used in this study. Color information including average gray-level intensities in RGB color space was selected to classify chicken livers. Image areas including fat band area and total area were measured on chicken heart. A feature index defined as the ratio of heart's fat band area to total heart area was used for classification of chicken hearts. Statistical analysis (Dunnnett t-test) was performed using SAS 6.12 (SAS Institute Inc., Cary, N.C.) to evaluate the feature selection.

FEATURE CLASSIFICATION

Feature classification is a process of grouping similar objects. A classifier is the inference engine to carry out the pattern classification task. Conventional classifier design involves clustering training samples and associating clusters with given classes. Due to the lack of an effective way of defining the boundaries among clusters, the computational complexity is increased when the number of features used for classification increases.

Fuzzy classification, on the other hand, allows the boundary between two neighboring classes to form an overlapping area, so that a feature has partial membership in each class. This provides a simple representation of the potentially complex partition of the feature space.

The fuzzy classifier can be described by a set of fuzzy if-then rules. Each fuzzy inference rule in the rule base can be represented as a conditional statement in the form of:

$$\begin{aligned} \text{If } & x_{p1} \text{ is } A_i \text{ and } x_{p2} \text{ is } B_i \text{ and } \dots \text{ and } x_{pn} \text{ is } Z_i \\ \text{Then } & x_p = (x_{p1}, \dots, x_{pn}) \text{ belongs to class } C_k \end{aligned} \quad (1)$$

where $x_p = (x_{p1}, \dots, x_{pn})$ are the features of pattern p ; A_i, B_i, \dots, Z_i are linguistic terms characterized by appropriate membership functions; $C_k, k = 1, 2, \dots, n$, are the classes. For example, applying an appropriate input feature space partition, a two-class (normal vs airsacculitis) liver classifier can be formulated. Figure 1 illustrates how the two-dimensional input space (x_1 : mean red brightness value; x_2 : mean green brightness value) is partitioned into six fuzzy regions, each of which is governed by a fuzzy if-then rule. The following 5 rules can be generated from the initial fuzzy partitions shown in figure 1.

- R1: If x_1 is small and x_2 is small then $x_p = (x_1, x_2)$ belongs to normal.
- R2: If x_1 is medium and x_2 is small then $x_p = (x_1, x_2)$ belongs to normal.
- R3: If x_1 is medium and x_2 is large then $x_p = (x_1, x_2)$ belongs to airsacculitis.
- R4: If x_1 is large and x_2 is small then $x_p = (x_1, x_2)$ belongs to airsacculitis.

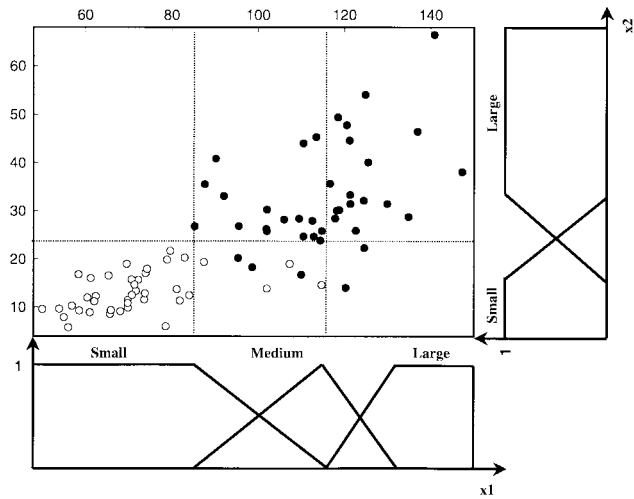


Figure 1—Fuzzy partition with six subspaces (closed and open circles represent the given pattern from airsacculitis and normal livers, respectively).

R5: If x_1 is large and x_2 is large then $x_p = (x_1, x_2)$ belongs to airsacculitis.

Based on the result of pattern matching between rule antecedents and input features, a number of fuzzy rules are triggered in parallel with various values of firing strength. The fuzzy inference engine, employing a combination of max and min operations, can then be applied to determine the level of certainty for pattern classification.

$$\mu_{CLASS}(C_k) = \max \min[\mu_{F1i}(x_{P1}), \mu_{F2j}(x_{P2}), \dots, \mu_{Fnk}(x_{Pn})] \quad (2)$$

where $\mu_{CLASS}(C_k)$ are the output membership grades for individual classes; $\mu_{F1i}(x_{P1}), \mu_{F2j}(x_{P2}), \dots, \mu_{Fnk}(x_{Pn})$ are the membership grades for the input features. The minimum operator is used to limit the certainty of the overall condition to that of the least certain observation. If the same characterization is prescribed by more than one selected rule, its certainty is set to the maximum of the individual rules. For example, assume that the red brightness (feature 1) belongs to R12 (medium) and R13 (large), and the green brightness (feature 2) belongs to G21 (small) and G22 (large) with corresponding membership grades, the output membership grades for the fuzzy classifier can be determined as follows:

$$\begin{aligned} \mu_{CLASS}(\text{normal}) &= \max [\min\{\mu_{R12}, \mu_{G21}\}, \\ &\quad \min\{\mu_{R12}, \mu_{G22}\}, \min\{\mu_{R13}, \mu_{G21}\}, \\ &\quad \min\{\mu_{R13}, \mu_{G22}\}] \\ \mu_{CLASS}(\text{air-sac}) &= \max [\min\{\mu_{R12}, \mu_{G21}\}, \\ &\quad \min\{\mu_{R12}, \mu_{G22}\}, \min\{\mu_{R13}, \mu_{G21}\}, \\ &\quad \min\{\mu_{R13}, \mu_{G22}\}] \end{aligned} \quad (3)$$

The classifier activates by selecting the one with maximum output membership grade, i.e., winner-take-all-interpretation.

NEURO-FUZZY CLASSIFIER

Fuzzy inference provides the possibility to transform linguistic descriptions of data into feature space partition to form a set of fuzzy rules in which a simple reasoning process can be carried out. However, if the membership functions are found to be unfit, then heuristic tuning (an unsystematic approach) has to be applied. In many pattern classification problems, no prior knowledge about the data is available, so that neither linguistic rules nor fuzzy reasoning can be effectively applied.

A neuro-fuzzy classifier, illustrated in figure 2, was used to solve these problems using the shareware NEFCLASS developed by Nauck and Kruse (1995). This classifier can be viewed as a special, three-layer, feed-forward neural network. The pattern features are fed into the input layer. The units of the second (hidden) layer represent the fuzzy rules, and the third layer consists of output units, one for each class. The fuzzy sets are represented as fuzzy weights on the connections from the input to the hidden layer. The learning procedure is divided into two phases. Phase I of the learning process is designed to discover the fuzzy rules. A fuzzy rule is created for a given pattern by finding the combination of fuzzy sets, in which each yields the highest degree of membership for the respective input feature. If this combination is not identical to the antecedents of an already existing rule, a new rule is created. After all patterns have been processed, the fuzzy inference rules are found by ranking the rules on the number of correct classifications they are involved in, and the first N rules are kept.

After the rule base is created, the second learning phase involves adapting the input membership functions. The signal flow for the fuzzy sets learning procedure consists of two passes: forward and backward pass. In the forward pass, input patterns go forward with computing the activation of each rule node using the t-norms (min) operation, and the activation of each output unit through the t-conorms (max) operation. After evaluating the output vectors, the signals keep going one more step for error calculation. Then the measured signal errors propagate backward from the output end toward the input end, and the parameters in the premise part (shape of membership functions) are updated by the delta learning rule (Widrow

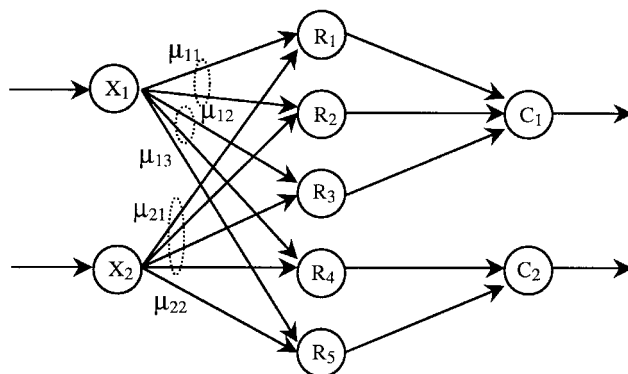


Figure 2—A neuro-fuzzy system with two inputs, five rules, and two output classes.

and Hoff, 1960). Usually the training process is terminated when the error reaches a predefined small value and/or a certain number of iterations have elapsed.

At the end of the learning processes we can interpret the structure of the network. The remaining rule nodes identify the fuzzy if-then rules that are necessary for feature space partition. The fuzzy weights represent the membership functions that describe the linguistic values of the input data pattern.

CONFIGURATION OF NEURO-FUZZY CLASSIFIERS

The neuro-fuzzy systems were applied to separate poultry viscera into classes. The data set contains 160 patterns, which belongs to four different classes: normal, airsacculitis, cadaver, and septicemia. For the neuro-fuzzy learning process the data set was randomly split in half, and the patterns were ordered alternately within the training and validation data sets. A cross validation scheme that contains the remaining 50% of data was used for model validation. Two sets of neuro-fuzzy models that utilized features extracted from color viscera images were examined for the classification of chicken livers and hearts. A unified neuro-fuzzy model with combined features from chicken livers and hearts was tested for poultry viscera classification.

RESULTS AND DISCUSSION

FEATURE ANALYSIS

Features Selected for Classification of Chicken Livers. The red, green, and blue mean brightness values were calculated from color liver images. Table 1 shows the color feature values for normal, airsacculitis, septicemia, and cadaver livers. Based on the experiment-wise type I error rate, Dunnett t-tests were performed to determine whether the mean responses for the populations of airsacculitis, septicemia, and cadaver livers differed from that for the normal (control) livers. Table 2 summarizes the comparisons of mean brightness values for airsacculitis, septicemia, and cadaver livers to the control. The Dunnett criterion for a two-sided test was computed by $D(3, 0.01) = 10.575$ when the mean red brightness value between normal livers and the other livers were compared. The differences ($|\bar{y}_i - \bar{y}_c|$) for airsacculitis and cadaver livers exceed the minimum significant difference calculated by $D(3, 0.01) = 10.575$. The test statistic indicates that the mean red brightness value for normal livers was significantly different from airsacculitis and cadaver livers. For the green color space response, the differences for airsacculitis and cadaver livers exceeded the minimum significant difference [$D(3, 0.01) = 4.4477$]. However, there was no significant difference ($|\bar{y}_i - \bar{y}_c| = 0.216$) between normal and septicemia livers. For the blue color

Table 1. Mean and standard deviation of color features for the normal, airsacculitis, septicemia, and cadaver livers

Sample	Number	Red		Green		Blue	
		Mean	S.D.	Mean	S.D.	Mean	S.D.
Normal	40	71.8	13.9	13.2	4.1	8.2	2.7
Airsacculitis	40	114.4	14.2	32.6	10.8	25.4	10.6
Septicemia	40	74.9	20.1	13.4	5.6	7.9	3.8
Cadaver	40	45.9	14.8	6.7	4.1	3.7	2.3

Table 2. Results of the Dunnett t-tests comparing the mean brightness values in the red, green, and blue color space for the normal livers to that of other livers

Liver Types Comparison	Difference Between Red Mean Values $ \bar{y}_i - \bar{y}_c $ *	Difference Between Blue Mean Values $ \bar{y}_i - \bar{y}_c $	Difference Between Green Mean Values $ \bar{y}_i - \bar{y}_c $
	Normal vs air-sac	42.6	19.4
Normal vs septicemia	3.1	0.2	0.3
Normal vs cadaver	25.9	6.5	4.5

* $|\bar{y}_i - \bar{y}_c|$: The absolute value of the mean R, G, and B differences between normal (y_c) livers and the other liver types (y_i).

NOTE: For the two-sided alternative with $H_0: \mu_i = \mu_c$ vs $H_a: \mu_i \neq \mu_c$; reject the null hypothesis if $|\bar{y}_i - \bar{y}_c| > D(k, \alpha)$ where k is the number of other liver types and α is Type I error rate.

space response, the differences for airsacculitis and cadaver livers exceeded the minimum significant difference [$D(3, 0.01) = 3.1383$]. A similar result also showed no significant difference ($|\bar{y}_i - \bar{y}_c| = 0.298$) between normal and septicemia livers when mean blue brightness values were used.

Table 3 summarizes the analysis of variance performed to the composite RGB images. The F test for the four liver types is 128.4, which is significant at the 1% significance level. The data indicates that there is a considerable difference among the four liver types when composite RGB liver images were compared. Dunnett's t-tests were performed to compare individual liver types (i.e., airsacculitis, septicemia, and cadaver) to the normal livers. The minimum significant difference of 5.032 was found when composite RGB brightness values between normal livers and the other liver types were compared. Similar results were also found that there were significant differences for normal versus airsacculitis ($|\bar{y}_i - \bar{y}_c| = 26.402$) and normal versus cadaver ($|\bar{y}_i - \bar{y}_c| = 17.308$), but no significant difference ($|\bar{y}_i - \bar{y}_c| = 1.004$) between normal and septicemia livers. The inference drawn from the test statistics indicates that features in RGB color space could be effectively used for differentiating normal livers from airsacculitis and cadaver livers. However, the color information is insufficient to differentiate between normal and septicemia livers.

Features Selected for Classification of Chicken Hearts. The feature index defined as the ratio of chicken heart's fat band area to total chicken heart area was calculated for chicken hearts classification. Table 4 summarizes the analysis of variance performed on the feature index measured from chicken heart images. The F

Table 3. Composite RGB liver images data ANOVA

Source of Variance	DF	Sum of Squares	Mean Squares	F Value	Pr > F
Between livers	3	31661.8585	10553.9528	182.40	0.0001
Within livers or error	156	9026.2554	57.8606		
Total	159	40688.1139			

Note: The probability of a type I error is designated as $\alpha = 1\%$.

Table 4. Feature index measured from heart images data ANOVA

Source of Variance	DF	Sum of Squares	Mean Squares	F Value	Pr > F
Between livers	3	6.4808	2.1603	222.43	0.0001
Within livers or error	156	1.5151	0.0097		
Total	159	7.9959			

NOTE: The probability of a type I error is designated as $\alpha = 1\%$.

test value (222.4) is significant at the 1% significance level for the four chicken heart types. The data shows there are significant differences between the four heart types being compared. Dunnett t-tests were performed to assess where the differences among populations of normal hearts versus airsacculitis, cadaver, and septicemia hearts really occur. Table 5 shows the results of significant tests among the four heart types. The normal chicken hearts differed significantly from the airsacculitis ($|\bar{y}_i - \bar{y}_c| = 0.372$) and the septicemia ($|\bar{y}_i - \bar{y}_c| = 0.1685$) hearts. However, there was no significant difference ($|\bar{y}_i - \bar{y}_c| = 0.042$) between normal and cadaver hearts when the ratio areas of chicken hearts were compared. The test statistics indicate that the feature index measured from chicken heart images can be applied to classify normal hearts from airsacculitis and septicemia hearts, but it cannot be effectively used for differentiating between normal and cadaver hearts.

CLASSIFICATION OF POULTRY VISCERA

Two-class Classification. Pairs of two-class classifiers (i.e., normal vs cadaver, normal vs airsacculitis, and normal vs septicemia) were constructed for establishing baseline information for viscera classifications. For the classification of chicken livers, the domains of three input features (i.e., red, green, and blue) were initially partitioned individually by three-equal distributed fuzzy sets. The membership functions were labeled as small, medium, and large for each input feature fuzzy set, resulting in maximum of 27 rules. Applying the rule learning procedure, the neuro-fuzzy classifier selected 14 fuzzy inference rules. The fuzzy set learning procedure was done for 500-epochs, and 6 out of 40 patterns from the training set (i.e., normal vs cadaver) were misclassified.

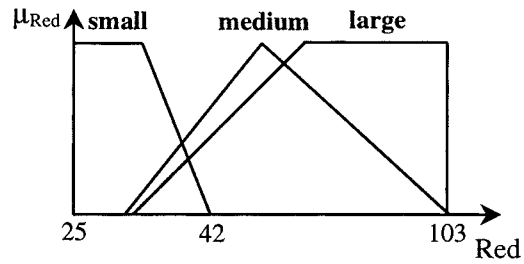
Figure 3 shows the fuzzy sets after the neuro-fuzzy learning process. The fuzzy sets “medium” for the green and blue input features were shifted and closely overlapped to the fuzzy sets “small”. This observation indicates that two fuzzy sets for each input feature should be sufficient.

The neuro-fuzzy classifier was re-trained with two fuzzy sets for each input feature. Two rules were created for

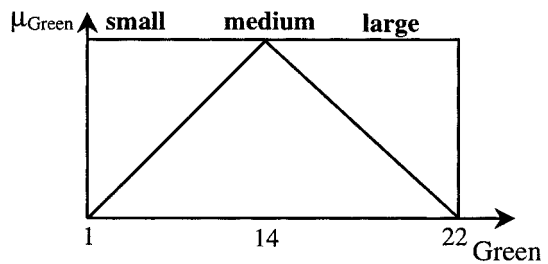
Table 5. Results of the Dunnett t-tests comparing the mean area ratio index value of the normal hearts to that of other hearts

Heart Types	Mean	Difference Between Means ($ \bar{y}_i - \bar{y}_c $)*	Different From Control?
Normal (control)	0.3225	N/A	N/A
Airsacculitis	0.6945	0.3720	Yes
Septicemia	0.1540	0.1685	Yes
Cadaver	0.2805	0.0420	No

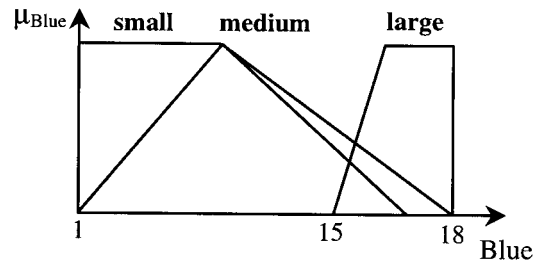
* Note that if the $|\bar{y}_i - \bar{y}_c|$ exceeds minimum significant difference = 0.0652, then the mean area ratio index value is different from that of normal (control).



(a)



(b)



(c)

Figure 3—Membership functions after the learning process: (a) red band, (b) green band, and (c) blue band.

distinguishing cadaver livers from normal livers. After learning, 4 out of 40 patterns from the training set were misclassified. The neuro-fuzzy classifier was cross-validated with the remaining 50% of data achieving a 87.5% accuracy. In a similar fashion, the second classifier was designed for distinguishing airsacculitis livers from normal livers. The classification accuracy for normal vs. airsacculitis was 95.0% for the training and 92.5% accuracy for the validation when color features in R, G, and B were used.

Table 6 compared the accuracy of neuro-fuzzy classifiers when the features of individual RGB and composite RGB were used for classification of chicken livers. The classification accuracy for two-class livers increased from 2.5% to 5.0% when the feature of composite RGB was used as input to the neuro-fuzzy models. This indicated composite RGB feature information can be effectively used for chicken liver classification.

For the classification of chicken hearts, a feature index defined as the ratio of heart’s fat band area to total heart area was used as input to the neuro-fuzzy model. A pair of two-class classifier (normal vs septicemia and normal vs airsacculitis) was designed using the same paradigm discussed previously. The classification accuracy for normal versus septicemia was 95.0% and 92.5% for the

Table 6. Performance evaluation of neuro-fuzzy models for two-class liver classification using individual R, G, B and composite RGB features

Classification	Accuracy* (%) (Training)	Accuracy* (%) (Validation)	Accuracy† (%) (Training)	Accuracy† (%) (Validation)
Normal vs cadaver	90.0	87.5	92.5	90.0
Normal vs air-sac	95.0	92.5	100	92.5

Samples: 40 livers (20 normal vs 20 cadaver and 20 normal vs air-sac) were used for training and the remaining 40 livers were used for validation.

* Using individual R, G, B brightness values as classification feature.

† Using composite RGB brightness values as classification feature.

training and validation, respectively. The classification accuracy to identify airsacculitis from normal chicken hearts was 100% for the training and 97.5% for the validation when the ratio area index of chicken hearts were used for the neuro-fuzzy model.

Three-class Classification. Based on information extracted from the previous two-class classifiers, three-class neuro-fuzzy classifiers were examined. Two classifiers were designed utilizing two sets of input features (i.e., R, G, B and composite RGB) for classification of chicken livers. The first classifier was initialized by six fuzzy sets (i.e., two for each input feature). The second classifier (i.e., composite RGB) was initialized by three fuzzy sets. The neuro-fuzzy rule learning process selected four inference rules for the first classifier and three inference rules for the second classifier. Table 7 summarizes the performance for three-class liver classification. The classification accuracy was 88.3% for the training and 83.3% for the validation when color features in R, G, and B were used. The classification accuracy increased 2% when composite RGB feature was used as input the neuro-fuzzy model.

Figure 4 shows the fuzzy sets and fuzzy inference rules for the classification of normal, airsacculitis, and septicemia. For the 120 patterns sampled the classification accuracy of 95.0% was achieved for the training and 93.3% accuracy for the validation.

Four-class Classification. In order to design the four-class classifier, feature information from chicken livers (composite RGB) and chicken hearts (area ratio index) were combined to form a set of parallel inputs to the neuro-fuzzy system. The fuzzy inference rules were devised initially by considering the reasoning discovered in two- and three-class models. These observations are: (1) a pattern belongs to cadaver if the value of composite RGB

Table 7. Performance Evaluation of neuro-fuzzy models for three-class liver classification using individual R, G, B and composite RGB features

Classification	Accuracy* (%) (Training)	Accuracy* (%) (Validation)	Accuracy† (%) (Training)	Accuracy† (%) (Validation)
Normal-cadaver-air-sac	88.3	83.3	90.0	85.0

Samples: 60 livers (20 normal, 20 cadaver, and 20 air-sac) were used for training and the remaining 60 livers were used for validation.

* Using individual R, G, B brightness values as classification feature.

† Using composite RGB brightness values as classification feature.

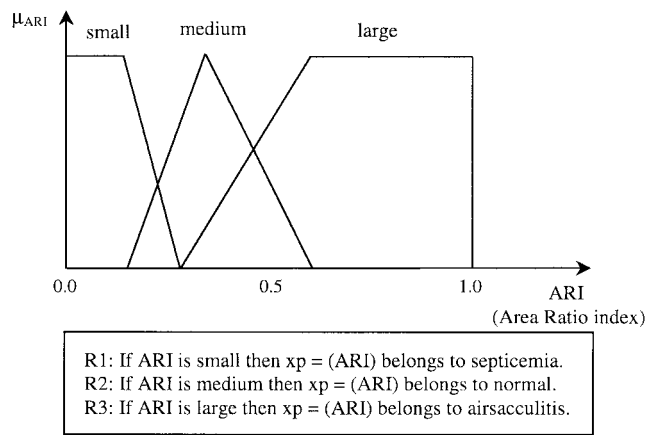


Figure 4—Membership functions and fuzzy inference rules for three-class heart classification.

is small; and (2) a pattern belongs to septicemia if the value of area ration index is small. The classifier was designed by six fuzzy sets (three for each input feature). With a prior knowledge, the neuro-fuzzy system generated seven fuzzy rules for the four-class model. For the 160 patterns sampled the classification accuracy of 86.2% was achieved for the training and 82.5% accuracy for the validation.

CONCLUSIONS

Based on the study reported in this article the following conclusions can be made.

1. Color viscera images provide useful feature information to identify individual condemned conditions of poultry viscera.
2. When neuro-fuzzy models using the color information were employed to separate chicken livers into normal, airsacculitis, and cadaver, the accuracy was 88.3% for the training data and 83.3% for the validation data. However, the color information was insufficient to differentiate between normal and septicemia livers.
3. When neuro-fuzzy models were employed to separate chicken hearts into normal, airsacculitis, and septicemia, the accuracy was 95.0% for the training data and 93.3% for the validation data. For this separation, only the spatial features (fat band to total area ratios) were found to be useful.
4. Combining features of chicken liver and heart, a generalized neuro-fuzzy model was designed to classify poultry viscera into four classes (normal, airsacculitis, cadaver, and septicemia). Both spectral and spatial information were used. The classification accuracy was 86.3% for training and 82.5% for validation.

In this study, models were developed to maximize total accuracy. In an on-line implementation, a differentiation between Type I error (economic loss risk) and Type II error (public health risk) would have to be made. Adjustment of thresholds would then enable acceptable balancing of both types of risk. For instance, the model could be used to separate a line into one with virtual certainty of normal chickens and one with a majority of abnormal chickens.

Manual inspection could then concentrate on the second line, resulting in a more efficient allocation of manpower.

REFERENCES

- Chen, Y. R., and D. R. Massie. 1993. Visible/Near-infrared reflectance and interactance spectroscopy for detection of abnormal poultry carcasses. *Transactions of the ASAE* 36(3): 863-869.
- Chen, Y. R., R. W. Huffman, and B. Park. 1996. Changes in the visible/NIR spectra of chicken carcasses in storage. *J. Food Process Engng.* 19: 121-134.
- Chen, Y. R., W. R. Hruschka, and H. Early. 1998a. On-line inspection of poultry carcasses using visible/near-infrared spectrophotometer, SPIE 3544: 146-155. Presented at the SPIE Conference on Pathogen Detection and Remediation for Safe Eating. Bellingham, Wash.
- Chen, Y. R., B. Park, R.W. Huffman, and M. Nguyen. 1998b. Classification of on-line poultry carcasses with back propagation neural networks. *J. Food Process Engng.* 21(Nov): 33-48.
- Daley, W., R. Carey, and C. Thompson. 1994. Real-time color grading and defect detection of food products. In *Optics in Agriculture, Forestry, and Biological Processing*, SPIE 2345: 403-411. Bellingham, Wash.
- Jang, J. R. 1993. ANFIS: Adaptive-Network-based Fuzzy Inference System. *IEEE Trans. Systems, Man, & Cybernetics* 23(3): 665-683.
- Mountney, M. 1987. U.S. Department of Agriculture standards for processed poultry and poultry products. In *The Microbiology of Poultry and Meat Products*, eds. F. E. Cunningham, and N. A. Cox, Ch. 6. New York, N.Y.: Academic Press, Inc.
- Nauck, D., and R. Kruse. 1995. NEFCLASS-a neuro-fuzzy approach for the classification of data. In *Proc. ACM Symp. on Applied Computing*, 26-28, Nashville, 26-28 Feb. New York, N.Y.: ACM Press.
- Park, B., and Y. R. Chen. 1996. Multispectral image co-occurrence matrix analysis for poultry carcasses inspection. *Transactions of the ASAE* 39(4): 1485-1491.
- Park, B., Y. R. Chen, and K. Chao. 1998. Multispectral imaging for detecting contamination in poultry carcasses. SPIE 3544: 110-120. Presented at the SPIE Conference on Pathogen Detection and Remediation for Safe Eating. Bellingham, Wash.
- Tao, Y., P. H. Heinemann, Z. Varghese, C. T. Morrow, and H. J. Sommer III. 1995. Machine vision for color inspection of potatoes and apples. *Transactions of the ASAE* 38(5): 1555-1561.
- Widrow, B., and M. E. Hoff. 1960. Adaptive switching circuits. In *IRE WESCON Convention Record*, 96-104.